

# A New Two-Dimensional Molybdenum(V) Nickel Phosphate Built Up of $[H_{18}(Mo_{16}O_{32})Ni_{16}(PO_4)_{26}(OH)_6(H_2O)_8]^{18-}$ Wheels

Charlotte du Peloux,<sup>†</sup> Anne Dolbecq,<sup>†</sup> Pierre Mialane,<sup>\*†</sup> Jérôme Marrot,<sup>†</sup> Eric Rivière,<sup>‡</sup> and Francis Sécheresse<sup>†</sup>

Institut Lavoisier, IREM, UMR 8637, Université de Versailles Saint-Quentin, 45 Avenue des Etats-Unis, 78035 Versailles, France, and Laboratoire de Chimie Inorganique, URA CNRS 420, Institut de Chimie Moléculaire d'Orsay, Université Paris-Sud, 91405 Orsay, France

Received July 31, 2002

The new molybdenum(V) nickel phosphate  $Na_6Ni_6[(Mo_2O_4)_8Ni_{16}(H_2PO_4)_4(HPO_4)_{10}(PO_4)_{12}(OH)_6(H_2O)_8] \cdot 66H_2O$  (**1**) was synthesized hydrothermally. The structure (orthorhombic, space group *Cccm*;  $a = 23.999(4)$ ,  $b = 36.595(6)$ ,  $c = 20.445(4)$  Å) was solved from single-crystal data. The framework structure of **1** consists of anionic inorganic sheets formed by the linkages of large polyoxomolybdate rings via nickel(II) octahedra. Charge-compensating sodium atoms are interleaved between the sheets. Magnetic studies of compound **1** revealed that among the 22 nickel(II) centers, 10 are interacting. The  $\chi_M T = f(T)$  curve can be fitted using the dinuclear expression appropriate to the HDVV isotropic exchange Hamiltonian  $H = -2JS_1 \cdot S_2$ , with  $S_1 = S_2 = 1$  and  $J = -24.1$  cm<sup>-1</sup>, showing that nickel is antiferromagnetically coupled within  $Ni_2$  pairs.

## Introduction

Polyoxometalates form an important class of materials that are attractive for their potential applications ranging from catalysis to medicine.<sup>1</sup> Molybdenum phosphates incorporating transition metals are interesting because they combine the properties of the polyoxomolybdates and those of the metal phosphates (magnetic properties, microporosity)<sup>2</sup> to form multipropertied materials. Furthermore, the combined use of transition metals and phosphate ligands allow one to connect Mo fragments into large clusters, forming eventually extended solid frameworks. The usual room-temperature aqueous synthetic conditions have afforded so far only a few molecular molybdenum(V) phosphates,<sup>3</sup> while one-pot hydrothermal techniques have proved to favor the formation

of multidimensional frameworks. The  $[P_4Mo_6O_{28}(OH)_3]^{9-}$  anion, with various degrees of protonation, is the most often encountered building unit in the reduced molybdenum phosphates,<sup>4</sup> but we have shown recently that two layered molybdenum(V) cobaltophosphates  $[(Mo_2O_4)_8(HPO_4)_{14}(PO_4)_{10}(Co_{22}Cl_2(H_2O)_{42})] \cdot 28H_2O$  (**2**) and  $[(Mo_2O_4)_8(HPO_4)_{14}(PO_4)_{10}(Co_{19}Na_4(H_2O)_{34})] \cdot 14H_2O$  (**3**), containing the unprecedented large structural group  $[(Mo_2O_4)_8(HPO_4)_{14}(PO_4)_{10}Co_{16}(H_2O)_{20}]^{10-}$ , could be synthesized hydrothermally.<sup>5</sup> These two compounds differ from the connection of the anionic wheels which occurs either by dimers of Co octahedra or by Co tetrahedra, depending of the pH of the synthesis. Attempts to obtain the analogous compound with Ni(II) in place of Co(II) has led to the two-dimensional compound  $Na_6Ni_6[(Mo_2O_4)_8Ni_{16}(H_2PO_4)_4(HPO_4)_{10}(PO_4)_{12}(OH)_6(H_2O)_8] \cdot 66H_2O$  (**1**). **1** differs from the previously described compounds **2** and **3**, showing variations both in the constitution of the building unit and in the linkage of the anionic rings.

## Experimental Section

A mixture of  $Na_2MoO_4 \cdot 2H_2O$  (0.94 g, 3.90 mmol), Mo (0.060 g, 0.62 mmol), 8 M  $H_3PO_4$  (1.06 mL, 8.44 mmol),  $NiCl_2 \cdot 6H_2O$  (0.88 g, 3.70 mmol), and water (4 mL) was stirred and the pH

\* To whom correspondence should be addressed. E-mail: mialane@chimie.uvsq.fr.

<sup>†</sup> Université de Versailles Saint-Quentin.

<sup>‡</sup> Université Paris-Sud.

- (1) See for example the following special issue: *Chem. Rev.* **1998**, *98*, 1–390.
- (2) (a) Cheetham, A. K.; Férey, G.; Loiseau, T. *Angew. Chem., Int. Ed.* **1999**, *38*, 3268. (b) Guillou, N.; Gao, Q.; Forster, P. M.; Chang, J.-S.; Noguès, M.; Park, S.-E.; Férey, G.; Cheetham, A. K. *Angew. Chem., Int. Ed.* **2001**, *40*, 2831.
- (3) (a) Dolbecq, A.; Cadot, E.; Eisner, D.; Sécheresse, F. *Inorg. Chim. Acta* **2000**, *300–302*, 151. (b) Cadot, E.; Salignac, B.; Loiseau, T.; Dolbecq, A.; Sécheresse, F. *Chem.—Eur. J.* **1999**, *5*, 3390. (c) Cadot, E.; Dolbecq, A.; Salignac, B.; Sécheresse, F. *Chem.—Eur. J.* **1999**, *5*, 2396. (d) Du Peloux, C.; Mialane, P.; Dolbecq, A.; Marrot, J.; Sécheresse, F. *Angew. Chem., Int. Ed.* **2002**, *41*, 2808.

(4) See for a review on the reduced molybdenum phosphates the following: Haushalter, R. C.; Mundi, L. A. *Chem. Mater.* **1992**, *4*, 31.

(5) Du Peloux, C.; Dolbecq, A.; Mialane, P.; Marrot, J.; Rivière, E.; Sécheresse, F. *Angew. Chem., Int. Ed.* **2001**, *40*, 2455.

**Table 1.** Crystallographic Data for  $\text{Na}_6\text{Ni}_6(\text{Mo}_2\text{O}_4)_8\text{Ni}_{16}(\text{H}_2\text{PO}_4)_4(\text{HPO}_4)_{10}(\text{PO}_4)_{12}(\text{OH})_6(\text{H}_2\text{O})_8 \cdot 66\text{H}_2\text{O}$  (**1**)

formula	$\text{H}_{172}\text{Mo}_{16}\text{Na}_6\text{Ni}_{22}\text{O}_{216}\text{P}_{26}$
<i>M</i>	7399.2
cryst system	orthorhombic
space group	Cccm
<i>a</i> /Å	23.999(4)
<i>b</i> /Å	36.595(6)
<i>c</i> /Å	20.445(4)
<i>V</i> /Å <sup>3</sup>	17956(5)
<i>Z</i>	4
$\mu/\text{mm}^{-1}$	3.721
reflens collcd	61 917
unique data ( <i>R</i> <sub>int</sub> )	12 560 (0.1140)
params	741
<i>R</i> <sub>1</sub> <sup>a</sup> , <i>wR</i> <sub>2</sub> <sup>b</sup> [ <i>I</i> > 2σ( <i>I</i> )]	0.0753, 0.1993

<sup>a</sup>  $R_1 = (\sum |F_o| - |F_c|) / \sum |F_c|$ . <sup>b</sup>  $wR_2 = [(\sum w(F_o^2 - F_c^2)^2) / (\sum w(F_o^2)^2)]^{1/2}$  with  $1/w = \sigma^2 F_o^2 + (aP)^2 + bP$  and  $a = 0.0737$  and  $b = 745.10$ .

adjusted to 3.3 with 1 M HCl. The resulting suspension was sealed in a 23 cm<sup>3</sup> Teflon-lined reactor which was kept at 130 °C for 216 h. Orange parallelepipedic crystals of **1** were separated by sonication and decantation from an unidentified powder and washed with water (32% yield, based on total Mo). Anal. Calcd for  $\text{H}_{172}\text{Ni}_{22}\text{Mo}_{16}\text{Na}_6\text{O}_{216}\text{P}_{26}$ : Ni, 17.44; Mo, 20.73; Na, 1.86; P, 10.89. Found: Ni, 17.90; Mo, 20.73; Na, 1.86; P, 10.98. IR for **1** (cm<sup>-1</sup>):  $\bar{\nu}$  515 (m), 548 (m), 584 (m); metal oxygen stretching region, 727 (w), 761 (m), 963 (s); phosphorus oxygen stretching region, 1068 (s), 1111 (s).

An orange crystal (0.20 × 0.20 × 0.06 mm) was analyzed with a Siemens SMART three-circle diffractometer equipped with a CCD bidimensional detector using Mo K $\alpha$  monochromatized radiation ( $\lambda = 0.71073$  Å). Details of the data collection as well as relevant crystallographic data are reported in Table 1. Data reduction was performed with the SAINT software. The absorption correction was based on multiple and symmetry-equivalent reflections in the data set using the SADABS program<sup>6</sup> based on the method of Blessing.<sup>7</sup> The structures were solved by direct methods and refined by full-matrix least squares using the SHELX-TL package.<sup>8</sup> The disordered oxygen and sodium atoms have been refined isotropically. Selected bond distances are listed in Table 2.

Magnetic susceptibility measurements were carried out with a Quantum Design SQUID magnetometer. The independence of the susceptibility value with regard to the applied field was checked at room temperature.

## Results and Discussion

**Synthesis.** Reaction of sodium molybdate with Mo metal as reducing agent, phosphoric acid, and nickel(II) chloride afforded with a moderately good yield orange parallelepipedic crystals of **1**, suitable for single-crystal X-ray diffraction analysis. The pH of the reacting solution is crucial for the formation of crystals since **1** only forms around pH = 3.3. Besides, a quite long heating period is necessary to induce the formation of **1**, probably because at the heating temperature (130 °C) the reduction of Mo(VI) ions by metallic Mo to produce Mo(V) centers is slower than at the higher temperatures (180 °C) usually used for the synthesis of reduced molybdenum phosphates. The single-crystal

**Table 2.** Selected Bond Lengths (Å) in  $\text{Na}_6\text{Ni}_6(\text{Mo}_2\text{O}_4)_8\text{Ni}_{16}(\text{H}_2\text{PO}_4)_4(\text{HPO}_4)_{10}(\text{PO}_4)_{12}(\text{OH})_6(\text{H}_2\text{O})_8 \cdot 66\text{H}_2\text{O}$  (**1**)

Mo1—O52	1.678(3)	Ni4—O28	2.121(3)
Mo1—O2	1.957(3)	Ni4—O38	2.214(3)
Mo1—O1	1.980(3)	Ni4—Ni4	3.261(1)
Mo1—O4	2.059(3)	Ni5—O35	2.036(2)
Mo1—O3	2.083(3)	Ni5—O34	2.067(4)
Mo1—O5	2.191(3)	Ni5—O36	2.069(3)
Mo1—Mo4	2.5981(6)	Ni5—Ni5	3.139(1)
Mo2—O9	1.677(3)	Ni6—O40	1.953(4)
Mo2—O12	1.936(3)	Ni6—O44	1.981(4)
Mo2—O10	1.950(3)	Ni6—O56	2.099(9)
Mo2—O6	2.047(3)	Ni6—O57	2.142(10)
Mo2—O7	2.060(3)	Ni7—O60	2.047(8)
Mo2—O8	2.415(2)	Ni7—O47	2.061(7)
Mo2—Mo3	2.5919(6)	Ni8—O59	1.788(9)
Mo3—O19	1.685(3)	Ni8—O37	1.957(4)
Mo3—O12	1.963(3)	Ni8—O49	2.157(8)
Mo3—O10	1.982(3)	Ni8—O55	2.257(9)
Mo3—O11	2.071(3)	Ni8—O50	2.204(12)
Mo3—O17	2.092(3)	Ni8—O48	2.203(4)
Mo3—O18	2.198(3)	P1—O37	1.502(4)
Mo4—O13	1.697(3)	P1—O25	1.548(4)
Mo4—O2	1.943(3)	P1—O6	1.544(3)
Mo4—O1	1.945(3)	P2—O18	1.531(3)
Mo4—O15	2.034(3)	P2—O30	1.543(4)
Mo4—O14	2.037(3)	P2—O8	1.556(4)
Mo4—O20	2.380(2)	P3—O29	1.521(4)
Ni1—O16	2.004(3)	P3—O7	1.532(3)
Ni1—O51	2.025(3)	P3—O35	1.539(4)
Ni1—O1	2.049(3)	P4—O5	1.546(3)
Ni1—O21	2.065(3)	P4—O51	1.557(4)
Ni1—O23	2.081(3)	P4—O20	1.591(4)
Ni1—O24	2.145(3)	P5—O3	1.527(3)
Ni1—Ni1	2.811(1)	P5—O21	1.528(3)
Ni1—Ni3	2.975(1)	P5—O17	1.537(3)
Ni2—O12	2.040(3)	P5—O39	1.565(3)
Ni2—O26	2.068(3)	P6—O23	1.517(4)
Ni2—O22	2.081(3)	P6—O40	1.528(4)
Ni2—O25	2.081(3)	P6—O15	1.550(3)
Ni2—O28	2.090(3)	P7—O28	1.524(3)
Ni2—O27	2.099(3)	P7—O4	1.525(3)
Ni2—Ni2	3.196(1)	P7—O11	1.540(3)
Ni2—Ni4	3.179(1)	P7—O41	1.555(3)
Ni3—O30	2.032(3)	P8—O42	1.507(4)
Ni3—O31	2.036(3)	P8—O26	1.541(3)
Ni3—O21	2.044(3)	P8—O43	1.596(4)
Ni3—O10	2.080(3)	P9—O44	1.500(5)
Ni3—O29	2.093(3)	P9—O14	1.547(3)
Ni3—O24	2.151(3)	P9—O38	1.551(5)
Ni3—Ni3	2.827(1)	P10—O16	1.527(4)
Ni4—O32	2.043(3)	P10—O45	1.537(4)
Ni4—O33	2.057(4)	P10—O31	1.554(3)
Ni4—O2	2.067(3)	P10—O46	1.585(4)
Ni4—O26	2.112(3)		

diffraction analysis has revealed a complex structure based on large anionic rings.

**Structure Description.** The structural building unit in **1** (Figure 1) can be described as a centrosymmetric ionic ring containing four tetramers of molybdenum(V) and four tetramers of nickel(II), encapsulating a central Ni octahedron located on an inversion center, at the intersection of a mirror plane and a C<sub>2</sub> axis. Valence bond calculations<sup>9</sup> have been applied on oxygen atoms to locate the protons of the phosphato groups (bond valence sums ( $\Sigma_s$ ) comprised in the range 1.01–1.15), the hydroxo ligands ( $0.69 \leq \Sigma_s \leq 1.05$ ), and the water molecules linked to the metal atoms ( $0.22 \leq \Sigma_s \leq 0.34$ ). The detailed formula of the wheel has thus been

(6) Sheldrick, G. M. *SADABS; program for scaling and correction of area detector data*; University of Göttingen: Göttingen, Germany, 1997.

(7) Blessing, R. *Acta Crystallogr., Sect. A* **1995**, *51*, 33.

(8) Sheldrick, G. M. *SHELX-TL version 5.03, Software Package for the Crystal Structure Determination*; Siemens Analytical X-ray Instrument Division: Madison, WI, 1994.

(9) Brese, N. E.; O'Keeffe, M. *Acta Crystallogr., Sect. B* **1991**, *47*, 192.

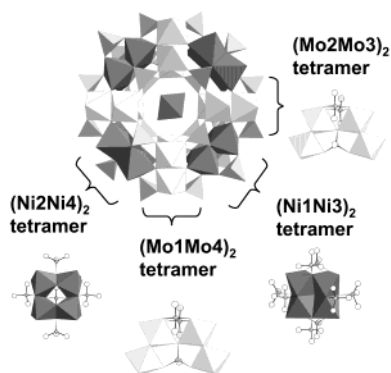


Figure 1. Polyhedral representation of the building unit in **1**.

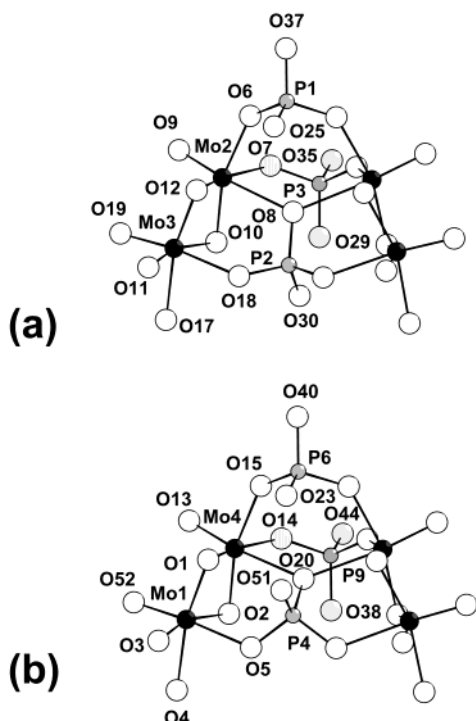


Figure 2. Ball and stick view with atom-labeling scheme of the  $(\text{Mo}_2\text{Mo}_3)_2$  tetramer (a) and the  $(\text{Mo}_1\text{Mo}_4)_2$  tetramer (b). A mirror plane intersects the  $(\text{Mo}_2\text{Mo}_3)_2$  tetramer in P1, P2, and P3 and the  $(\text{Mo}_1\text{Mo}_4)_2$  tetramer in P4, P6, and P9.

stated as  $[(\text{Mo}_2\text{O}_4)_8(\text{H}_2\text{PO}_4)_4(\text{HPO}_4)_{10}(\text{PO}_4)_{12}\text{Ni}_{16}(\text{OH})_6(\text{H}_2\text{O})_8]^{18-}$ . All metal atoms (Mo and Ni) display distorted octahedral coordinations (Table 2). As observed for most of the previously reported structures of reduced molybdates, the Mo(V) centers are dimerized<sup>10</sup> and form diamagnetic  $\{\text{Mo}_2(\mu\text{-O})_2\}$  pairs with Mo–Mo distances close to 2.6 Å (Table 2). Two nearly related tetramers of Mo (Figure 2), deriving from previously described oxomolybdenum clusters,<sup>11</sup> are present in the asymmetric unit. They are formed by the linkage of two  $\{\text{Mo}_2(\mu\text{-O})_2\}$  dimers by three phosphato groups through a  $\mu_3$ -oxygen (O20, O8 for tetramer  $(\text{Mo}_1\text{Mo}_4)_2$  and tetramer  $(\text{Mo}_2\text{Mo}_3)_2$ , respectively) and six  $\mu_2$ -oxygen atoms (O5, O14, O15 and O6, O7, O18 for tetramer

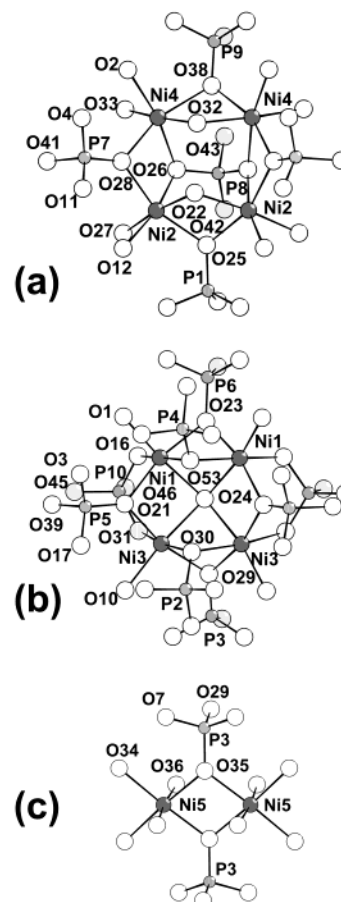
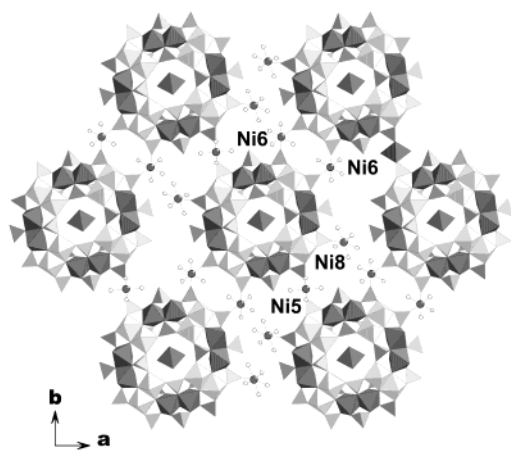


Figure 3. Ball and stick view with atom-labeling scheme of the  $(\text{Ni}_2\text{Ni}_4)_2$  tetramer (a), the  $(\text{Ni}_1\text{Ni}_3)_2$  tetramer (b), and the  $\text{Ni}_5\text{Ni}_5$  dimer (c). A mirror plane intersects the  $(\text{Ni}_2\text{Ni}_4)_2$  tetramer in P1, P8, and P9 and the  $(\text{Ni}_1\text{Ni}_3)_2$  tetramer in P2, P3, P4, and P6; the  $\text{Ni}_5\text{Ni}_5$  dimer is located at the intersection of two mirror planes.

$(\text{Mo}_1\text{Mo}_4)_2$  and tetramer  $(\text{Mo}_2\text{Mo}_3)_2$ , respectively) and are identical to those encountered in the constituting units of **2** and **3**. While in **2** and **3** only one kind of Co tetramer was encountered, in **1** two kinds of Ni tetramers can be distinguished, namely tetramer  $(\text{Ni}_2\text{Ni}_4)_2$  and tetramer  $(\text{Ni}_1\text{Ni}_3)_2$ . The overall symmetry of the wheel is thus lowered from  $C_{4v}$  for **2** and **3** to  $C_{2v}$  for **1**. The first kind of Ni tetramer (Figure 3a) is built of four coplanar edge-sharing Ni octahedra and is similar but not identical to the tetramers of Co in **2** and **3**. The Ni centers are located at the vertexes of a nearly regular square (Table 2) and are bridged through two hydroxo groups (O22, O32) and six  $\mu_3$ -oxygen atoms (O25, O26, O28, O38) of five distinct phosphato groups. The coordination sphere of each Ni is completed by one water molecule (O27, O33). The second Ni tetramer (Figure 3b) consists of four alternately edge- and face-sharing octahedra. The four coplanar Ni centers form a rectangle (Table 2) around a central  $\mu_4$ -OH ligand (O24) and are bridged by eight oxygen atoms (O21, O23, O29, O30, O31, O53) of eight phosphato groups. The central  $\mu_4$ -OH ligand (O24) is located 0.65 Å above the mean plane of the  $\text{Ni}_4$  group. The Ni–Ni distances in  $(\text{Ni}_1\text{Ni}_3)_2$  are significantly shorter than the Ni–Ni distances in the  $(\text{Ni}_2\text{Ni}_4)_2$  tetramer.

(10) Müller, A.; Kuhlmann, C.; Bögge, H.; Schmidtman, M.; Baumann, M.; Krickemeyer, E. *Eur. J. Inorg. Chem.* **2001**, 2271.

(11) Khan, M. I.; Chen, Q.; Salta, J.; O'Connor, C. J.; Zubieta, J. *Inorg. Chem.* **1996**, *35*, 1880.



**Figure 4.** View of the connecting scheme between the building groups in **1** with the labels of the Ni atoms anchored to the ring.

The geometry of the  $(\text{Ni1Ni3})_2$  tetramer is thus very close to that described for the  $\text{Ni}_4$  complex of a macrocyclic tetranucleating ligand with bridging acetato and methoxo ligands.<sup>12</sup> In particular, the Ni–Ni distances are similar and both compounds contain a central uncommon  $\mu_4$ -OH ligand.

Each wheel is surrounded by six other coplanar anionic rings. The connections are ensured by Ni5 and Ni6 octahedra through phosphato groups (Figure 4). Ni8 is a pendant disordered  $\text{Ni}(\text{H}_2\text{O})_5$  group. Ni6 forms disordered isolated Ni octahedra while two adjacent Ni5 octahedra share edges, forming a centrosymmetric Ni dimer (Figure 3c). The coordination sphere of Ni5 and Ni6 is constituted by two  $\mu_2$ -oxygen atoms of phosphato ligands and four water molecules. The connection of the wheels through Ni octahedra produces a two-dimensional framework to which Na counterions are anchored.

**Magnetic Properties.** The thermal dependence of  $1/\chi_M$  and  $\chi_M T$  for compound **1**, where  $\chi_M$  is the magnetic susceptibility per  $\text{Na}_6\text{Ni}_6[(\text{Mo}_2\text{O}_4)_8\text{Ni}_{16}(\text{H}_2\text{PO}_4)_4(\text{HPO}_4)_{10}(\text{PO}_4)_{12}(\text{OH})_6(\text{H}_2\text{O})_8]\cdot 66\text{H}_2\text{O}$  unit, is shown in Figure 5.<sup>13</sup> The  $\chi_M T$  curve exhibits a continuous decrease upon cooling from 300 K ( $\chi_M T = 25.75 \text{ cm}^3 \cdot \text{mol}^{-1} \cdot \text{K}$ ) to 2 K ( $\chi_M T = 7.46 \text{ cm}^3 \cdot \text{mol}^{-1} \cdot \text{K}$ ), characteristic of an antiferromagnetic behavior. Considering the distances between two nickel centers connected via O–P–O bridges, the shortest being of 4.993 Å between Ni3 and Ni5, the main interactions must occur from nickel octahedra sharing edges ( $d_{\text{Ni-Ni}} = 3.14$ – $3.26$  Å) or faces ( $d_{\text{Ni-Ni}} = 2.811$ – $2.975$  Å). Then, it follows that the 22 nickel centers can be formally divided in four tetrameric groups (two  $(\text{Ni1Ni3})_2$  and two  $(\text{Ni2Ni4})_2$  tetramers), one dimeric unit (the  $(\text{Ni5})_2$  dimer), and four monomeric

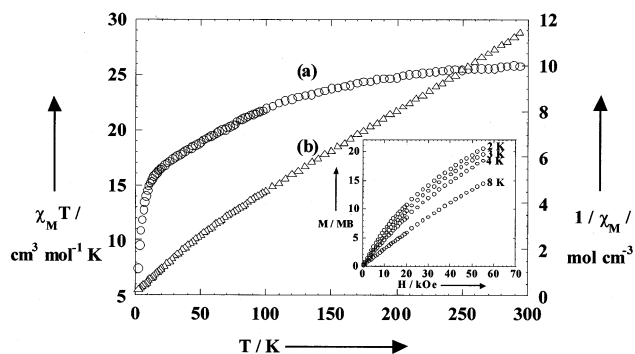


**Figure 5.** Thermal dependence of  $\chi_M T$  (a) and  $1/\chi_M$  (b) for **1**. Inset: Magnetization versus magnetic field at 2, 3, 4, and 8 K.

complexes (two Ni6 and two Ni8 octahedra). The magnetization as a function of the applied magnetic field has been measured at four different temperatures comprised between 2 and 8 K (Figure 5, inset). Clearly, it appears that the data cannot be interpreted by considering only four noncoupled nickel(II) cations ( $M = 20.5 \mu_B$  for  $H = 55 \text{ kOe}$  and  $T = 2 \text{ K}$ , for an expected value at saturation of  $M = 8 \mu_B$  assuming  $g = 2$ ) and implies that even metal centers with short  $\text{Ni} \cdots \text{Ni}$  distances are noncoupled. This phenomenon has been previously observed.<sup>14</sup> In the case of nickel(II) polynuclear complexes, it is assumed that the most important superexchange pathway is provided via the orbitals  $d_{x^2-y^2}$ . This implies that the influence of the nature of the axial ligands must be slight. Indeed, Hendrickson et al. reported two dimeric complexes  $\text{LNi}_2\text{Cl}_2$ <sup>15</sup> and  $\text{LNi}_2\text{py}_4$ <sup>16</sup> (L being a hexadentate macrocyclic ligand) for which  $J$  values were found to be  $-27$  and  $-23 \text{ cm}^{-1}$ , respectively.<sup>17</sup> Moreover, Robson et al. reported three tetrameric nickel(II) complexes, where in each case the four metal centers are enclosed in an imino/phenolato octadentate macrocyclic ligand, the nickel centers defining a distorted rectangle. It was then noticed that the magnetic data of these complexes can be fitted by considering a “pair of dimers” model, the use of a tetranuclear model, where three  $J$  values corresponding to dissimilar edges and diagonal interactions are introduced, being then superfluous. A unique  $J$  value close to  $-30 \text{ cm}^{-1}$  for each complex was then determined.<sup>18</sup> Enforced by these experimental observations, Murray proposed that if the equatorial ligands of each potentially interacting metal center belong to a unique plane, an antiferromagnetic coupling is expected, while no coupling can occur if noncoplanarity is observed (see Scheme 1). As mentioned above, the topology of the  $(\text{Ni1Ni3})_2$  tetrameric units of **1** (Figure 3b) is similar to that found for the tetrameric complexes reported by Robson et al. Indeed, a plane contains the atoms O1, O23, Ni1, O21, O24, Ni3, Ni10, and O29, while no unique plane

(12) Bell, M.; Edwards, A. J.; Hoskins, B. F.; Kachab, E. H.; Robson, R. *J. Am. Chem. Soc.* **1989**, *111*, 3603.

(13) As usual for nickel(II) compounds, a temperature-independent paramagnetic correction has been applied on the raw data ( $\chi_{\text{TP}} = 150 \times 10^{-6} \text{ cm}^3 \cdot \text{mol}^{-1} / \text{metal center}$ ). See for example: (a) Du, M.; Bu, X.-H.; Guo, Y.-M.; Zhang, L.; Liao, D.-Z.; Ribas, J. *Chem. Commun.* **2002**, 1478. (b) Pavlishchuk, V. V.; Kolotilov, S. V.; Addison, A. W.; Prushan, M. J.; Schollmeyer, D.; Thompson, L. K.; Goreshnik, E. A. *Angew. Chem., Int. Ed.* **2001**, *40*, 4734. The diamagnetic contribution to the magnetic susceptibility has been calculated using the relation  $\chi_D = -0.5 \times 10^{-6} M \text{ cm}^3 \cdot \text{mol}^{-1}$ , where  $M$  refers to the molecular weight of compound **1**.

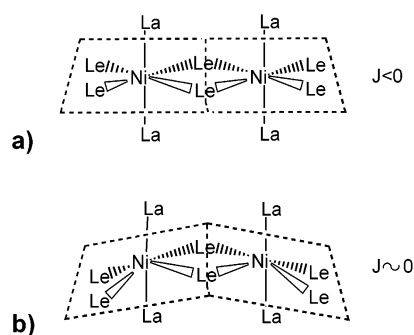
(14) (a) Cano, J.; De Munno, G.; Lloret, F.; Julve, M. *Inorg. Chem.* **2000**, *39*, 1611. (b) Nanda, K. K.; Das, R.; Thompson, L. K.; Venkatsubramanian, K.; Nag, K. *Inorg. Chem.* **1994**, *33*, 5934.

(15) Lambert, S. L.; Hendrickson, D. N. *Inorg. Chem.* **1979**, *18*, 2683.

(16) Spiro, C. L.; Lambert, S. L.; Smith, T. J.; Duesler, E. N.; Gagne, R. R.; Hendrickson, D. N. *Inorg. Chem.* **1981**, *20*, 1229.

(17) In the text, all the  $J$  values are given by considering the  $H = -2JS_1 \cdot S_2$  phenomenological Hamiltonian.

(18) Edwards, A. J.; Hoskins, B. F.; Kachab, E. H.; Markiewicz, A.; Murray, K. S.; Robson, R. *Inorg. Chem.* **1992**, *31*, 3585.

Scheme 1<sup>a</sup>

<sup>a</sup> (a) The equatorial ligands of each metal center belong to a unique plane ( $J < 0$ ). (b) The equatorial ligands of each metal center do not belong to a unique plane ( $J \approx 0$ ). (Le = equatorial ligand, La = axial ligand).

contains the equatorial planes of the Ni1...Ni1 and Ni3...Ni3 pairs. Furthermore, as the equatorial ligands of Ni2 and Ni4 centers do not belong to a unique plane, no coupling within the (Ni2Ni4)<sub>2</sub> tetramers is expected. It follows that only the four Ni1...Ni3 and the Ni5...Ni5 pairs are supposed to magnetically interact. Considering the  $1/\chi_M = f(T)$  curve between 200 and 300 K, a  $g_{av} = 2.25$  value has been determined. Then, the theoretical  $\chi_M T = f(T)$  curves corresponding to the 12 isolated nickel centers have been calculated and subtracted from that of the experimental data (Figure 6, inset). Assuming that the coupling constants  $J$  must be similar for the Ni1...Ni3 and the Ni5...Ni5 pairs,  $\chi_M T$  for the five coupled pairs could thus be expressed as follows:

$$\chi_M T = \frac{5N\beta^2 g^2}{k} \left[ \frac{10 + 2 \exp(-2x)}{5 + 3 \exp(-2x) + \exp(-3x)} \right]$$

$$x = \frac{2J}{kT}$$

Here the equation is relative to the HDVV isotropic exchange Hamiltonian  $H = -2JS_1 \cdot S_2$ . Considering that large ZFS parameters are found for nickel(II) centers, the curve has been fitted between 50 and 300 K (Figure 6).<sup>19</sup> The best fit has been obtained for  $g = 2.25$  and  $J = -24.3 \text{ cm}^{-1}$ . These values are consistent with those previously reported for nickel(II) polynuclear units, confirming that the coupling constant is much more dependent on the topology of the complex than on the nature of the bridging ligands.

In conclusion, a new two-dimensional nickel molybdenum phosphate, differing from the cobalto analogues, has been obtained. This shows that the two-dimensional structure is determined by the nature of the transition metal. Remarkably, even if the structure of **1** is complex, it has been possible to interpret the magnetic data with the phenomenological

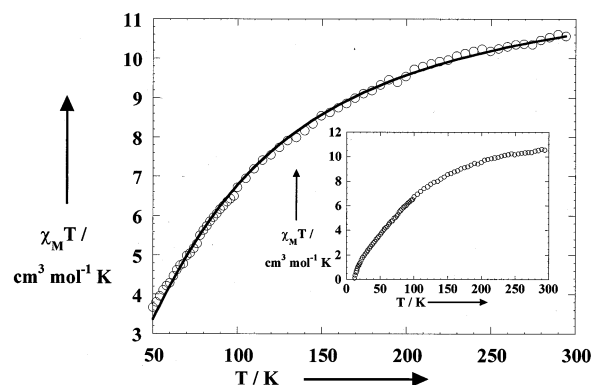


**Figure 6.** Calculated  $\chi_M T = f(T)$  curve corresponding to the 10 coupled nickel(II) centers between 50 and 300 K for **1**. The solid line was generated from the best fit parameters given in the text. Inset: Calculated  $\chi_M T = f(T)$  curve between 0 and 300 K corresponding to the 10 coupled nickel(II) centers.

Hamiltonian relative to dimeric pairs of nickel(II) centers. Indeed, among the 22 nickel(II) centers, only 10 are interacting, the remaining magnetic centers behaving as isolated centers even when Ni–Ni distances are short.

**Acknowledgment.** P.M. thanks Prof. Dr. T. Mallah for fruitful discussions on magnetic data interpretation.

**Supporting Information Available:** One X-ray crystallographic file, in CIF format, and three figures, showing the magnetization versus magnetic field curves at 2, 3, 4, and 8 K for **1** fitted with a law relative to the adapted ZFS phenomenological Hamiltonian, the deduced  $\chi_M T = f(T)$  curve corresponding to 12 isolated nickel centers, and the calculated  $\chi_M T = f(T)$  curve corresponding to the 10 coupled nickel(II) centers between 50 and 300 K fitted with the Van Vleck equation given in the text. This material is available free of charge via the Internet at <http://pubs.acs.org>.

IC0204880

- (19) Fits of the  $M = f(H)$  curves have been effectuated by considering the spin Hamiltonian  $H = \beta S \cdot [g] \cdot B + D[S_z^2 + 1/3S(S+1)] + E(S_x^2 - S_y^2)$  (see Supporting Information). The best fits have been obtained, assuming  $g = 2.25$ , for  $D = -10.2 \text{ cm}^{-1}$  and  $E/D = 0.159$ . Considering these values the contribution to the magnetic susceptibility of the monomeric Ni(II) species has been calculated and subtracted from the experimental  $\chi_M T = f(T)$  curve. As expected, the resulting calculated  $\chi_M T = f(T)$  curve, corresponding to only coupled nickel(II) centers, tends to  $\chi_M T = 0$  at 0 K. This curve has been fitted between 50 and 300 K by the isotropic exchange Hamiltonian  $H = -2JS_1 \cdot S_2$ . The best fit affords  $g = 2.25$  and  $J = -24.1 \text{ cm}^{-1}$ . These values are in very good agreement with the values given in the text, an expected result as the ZFS effect is nearly negligible above 50 K. Nevertheless, the obtained  $D$  value seems large. Moreover, the slight deviations between the calculated and experimental  $M = f(H)$  curves observed at high field are presumably due to the fact that very small interactions occur between metal centers which have been considered as isolated. Then, the treatment of the  $M = f(H)$  curves with a pure ZFS phenomenological Hamiltonian may be insufficient.